Contrib Mineral Petrol (1997) 129: 143–154

Thomas Stachel · Jeff W. Harris

Diamond precipitation and mantle metasomatism – evidence from the trace element chemistry of silicate inclusions in diamonds from Akwatia, Ghana

Received: 27 January 1996 / Accepted: 5 May 1997

Abstract Trace element concentrations in the four principal peridotitic silicate phases (garnet, olivine, orthopyroxene, clinopyroxene) included in diamonds from Akwatia (Birim Field, Ghana) were determined using SIMS. Incompatible trace elements are hosted in garnet and clinopyroxene except for Sr which is equally distributed between orthopyroxene and garnet in harzburgitic paragenesis diamonds. The separation between lherzolitic and harzburgitic inclusion parageneses, which is commonly made using compositional fields for garnets in a CaO versus Cr_2O_3 diagram, is also apparent from the Ti and Sr contents in both olivine and garnet. Titanium is much higher in the lherzolitic and Sr in the harzburgitic inclusions. Chondrite normalised REE patterns of lherzolitic garnets are enriched (10–20 times chondrite) in HREE (La_N/Yb_N = 0.02–0.06) while harzburgitic garnets have sinusoidal REE_N patterns, with the highest concentrations for Ce and Nd (2–8 times chondritic) and a minimum at Ho (0.2–0.7 times chondritic). Clinopyroxene inclusions show negative slopes with La enrichment 10–100 times chondritic and low Lu (0.1–1 times chondritic). Both a lherzolitic and a harzburgitic garnet with very high knorringite contents (14 and 21 wt% Cr_2O_3 respectively) could be readily distinguished from other garnets of their parageneses by much higher levels of LREE enrichment. The REE patterns for calculated melt compositions from lherzolitic garnet inclusions fall into the compositional field for kimberlitic-lamproitic and carbonatitic melts. Much more strongly fractionated REE patterns calculated from harzburgitic garnets, and low concentrations in Ti, Y, Zr, and Hf, differ significantly from known alkaline and carbonatitic melts and require a different agent. Equilibration temperatures for harzburgitic inclusions are generally below the C-H-O solidus of their paragenesis, those of lherzolitic inclusions are above. Crystallisation of harzburgitic diamonds from CO_2-bearing melts or fluids may thus be excluded. Diamond inclusion chemistry and mineralogy also is inconsistent with known examples of metasomatism by H_2O-rich melts. We therefore favour diamond precipitation by oxidation of CH_4-rich fluids with highly fractionated trace element patterns which are possibly due to "chromatographic" fractionation processes.

T. Stachel (✉)
Institut für Mineralogie, Universität Frankfurt,
Postfach 11 19 32, D-60054 Frankfurt, Germany

J.W. Harris
Department of Geology and Applied Geology,
University of Glasgow, Glasgow G12 8QQ, UK

Editorial responsibility: I. Parsons

Introduction

Here we present the first account of the abundance of REE (rare earth elements), HFSE (high field strength elements), and LILE (large ion lithophile elements) in garnet, ortho- and clinopyroxene, and olivine inclusions found as lherzolitic and harzburgitic parageneses in diamonds from Akwatia (Ghana). Such data provide insights into ancient (Richardson et al. 1984, 1993) metasomatism in lherzolitic and harzburgitic parts of the subcratonic lithospheric upper mantle. Equally importantly, these data may contribute to a better understanding of the environment of formation of diamond.

In all, twenty-four non-touching silicate inclusions were obtained from alluvial diamonds from Akwatia, in the Birim diamond field of Ghana. For the major element chemistry of these mineral inclusions and the physical characteristics of the host diamonds (nitrogen contents, nitrogen aggregation levels, carbon and nitrogen isotope signatures) see Stachel and Harris (1997).

Analytical method

Trace element analyses were carried out using the CAMECA IMS 4f ion microprobe with Charles Evans and Associates interface and

Table 1. Composition of silicate inclusions in diamonds from Akwatia. Electron microprobe analyses as oxides in wt%, ion microprobe analyses as elements in wt ppm. (*ND* not detected)

Mineral	Lherzolitic garnet	Clinopyroxene	Clinopyroxene	Lherzolitic olivine	Lherzolite garnet	Clinopyroxene	Harzburgitic garnet	Harzburgitic olivine	Harzburgitic garnet	Harzburgitic Orthopyroxene	Harzburgitic garnet	Harzburgitic Orthopyroxene
Sample	G4-3	G23-29	G41-69	G50-80	G50-82	G50-83	G103-104	G103-106	G104-107	G104-108	G111-122	G111-125
Assemblage	Garnet	Olivine1 2clinopyroxene	2clinopyroxene		2Garnet 2clinopyroxene, 2olivine		2 olivine	2Garnet	orthopyroxene	Garnet,	2 Garnet, 3orthopyroxene	
P_2O_5	–	< 0.03	–	< 0.03	< 0.03	< 0.03	< 0.02	< 0.02	< 0.02	< 0.02	< 0.02	< 0.02
SiO_2	39.6	54.8	54.6	41.0	41.5	54.4	42.2	41.2	41.8	58.0	42.3	57.5
TiO_2	0.10	< 0.03	< 0.03	< 0.03	0.20	0.05	< 0.02	< 0.02	< 0.02	< 0.02	< 0.02	< 0.02
Al_2O_3	13.3	0.81	0.77	< 0.02	19.0	0.85	19.8	0.02	19.0	0.58	18.0	1.19
Cr_2O_3	14.2	0.78	0.84	0.05	7.13	0.84	5.42	0.02	6.40	0.30	8.16	0.69
FeO	7.28	2.88	2.63	8.71	6.88	2.72	5.89	7.38	6.02	4.47	4.92	3.67
MnO	0.37	0.14	0.13	0.10	0.33	0.12	0.24	0.08	0.29	0.09	0.21	0.09
NiO	< 0.04	0.08	< 0.04	0.47	< 0.04	0.05	< 0.02	0.41	< 0.02	0.13	0.03	0.13
MgO	17.3	20.0	18.7	49.5	19.7	18.8	23.4	50.9	21.7	35.5	25.6	36.6
CaO	7.70	19.2	20.9	0.05	6.29	20.5	2.84	0.01	4.63	0.66	0.72	0.13
Na_2O	< 0.03	0.52	0.25	0.03	< 0.03	0.57	< 0.02	0.02	< 0.02	0.02	< 0.02	< 0.02
K_2O	< 0.02	0.10	0.72	< 0.02	< 0.02	0.10	< 0.01	< 0.01	< 0.01	< 0.01	< 0.01	< 0.01
Total	99.9	99.3	99.6	99.9	100.0	99.1	99.8	100.0	99.8	99.8	100.0	100.0
Ti	754.0	52.4	29.1	8.95	1073.	194.	17.9	0.59	24.2	4.69	47.3	9.50
Rb	0.23	ND	0.05	0.19	0.10	ND	0.03	0.24	0.05	0.16	0.20	0.08
Sr	5.47	386.	300.	0.33	0.39	79.4	2.83	0.62	3.35	3.64	3.07	3.30
Y	3.90	0.25	0.13	0.03	9.86	0.40	0.85	0.02	0.09	0.01	0.32	0.01
Zr	13.5	0.09	0.17	0.13	8.88	0.24	0.44	0.14	0.18	0.02	4.76	0.06
Nb	3.45	0.27	0.28	0.02	1.82	0.38	1.06	ND	0.74	0.06	0.69	0.01
Ba	0.04	0.34	11.6	0.04	0.02	6.36	0.01	0.04	0.02	0.05	0.03	0.03
La	2.08	3.22	26.4	0.00	0.15	3.48	0.19	0.01	0.73	0.03	0.32	0.00
Ce	5.79	12.7	51.5	0.01	0.53	4.26	1.46	0.02	4.00	0.09	2.42	0.03
Pr	0.60	2.18	4.07	0.00	0.09	0.40	0.24	0.00	0.45	0.01	0.51	0.01
Nd	2.08	8.48	9.77	0.01	0.92	1.73	0.93	0.01	0.74	0.02	2.56	0.02
Sm	0.41	0.39	0.44	0.02	0.56	0.30	0.11	0.01	0.02	0.01	0.35	0.01
Eu	0.13	0.05	0.04	0.00	0.26	0.13	0.03	ND	0.00	ND	0.09	ND
Gd	0.74	0.09	0.05	0.01	1.10	0.23	0.16	ND	ND	ND	0.28	0.00
Tb	0.10	0.02	0.03	ND	0.23	0.03	0.01	ND	ND	ND	0.04	0.00
Dy	0.83	0.19	0.04	ND	2.08	0.15	0.11	ND	ND	0.03	0.13	ND
Ho	0.17	0.01	0.00	0.00	0.42	0.03	0.03	ND	ND	ND	0.01	0.00
Er	0.43	0.06	0.08	0.01	1.30	0.04	0.23	ND	0.01	0.00	0.07	0.00
Yb	0.66			0.00	1.58		0.83	ND	0.13	0.02	0.05	ND
Lu	0.15	0.00	0.01	0.00	0.26	0.00	0.15	ND	0.03	0.00	0.03	0.00
Hf	0.49	ND	0.01	0.00	0.39	ND	0.02	ND	0.02	ND	0.10	0.03

Table 1 (*contd.*)

Mineral	Lherzolitic garnet	Orthopyroxene	Harzburgitic garnet	Orthopyroxene	Harzburgitic olivine	Harzburgitic olivine	Clinopyroxene	Lherzolitic olivine	Lhersolitic garnet	Orthopyroxene	Harzburgitic garnet	Harzburgitic garnet
Sample	G113-132	G119-146	G126-155	G126-157	G126-158	G127-160	G201-201	G201-202	G201-203	G209-215	G209-216	G303-305
Assemblage	Garnet 2 2olivine	Olivine orthopyroxene		2Garnet, 2olivine orthopyroxene		Olivine, chromite		Garnet, olivine clinopyroxene			Garnet, olivine orthopyroxene	Garnet olivine
P_2O_5	0.03	< 0.02	< 0.02	< 0.02	< 0.02	< 0.02	< 0.02	< 0.02	< 0.02	< 0.02	< 0.02	0.04
SiO_2	41.8	57.8	41.7	57.9	41.1	41.2	54.7	40.5	41.6	57.9	40.9	40.8
TiO_2	0.37	< 0.02	< 0.02	< 0.02	< 0.02	< 0.02	0.18	< 0.02	0.71	< 0.02	< 0.02	< 0.02
Al_2O_3	19.6	0.50	16.3	0.84	< 0.01	0.03	1.22	0.03	19.3	0.46	15.6	6.99
Cr_2O_3	5.38	0.30	10.2	0.60	0.05	0.03	0.69	0.06	4.32	0.35	11.2	20.6
FeO	5.68	4.39	5.93	4.29	7.16	6.31	2.72	9.46	7.00	4.31	6.20	6.73
MnO	0.23	0.12	0.27	0.10	0.11	0.10	0.11	0.17	0.33	0.12	0.28	0.29
NiO	< 0.02	0.16	0.02	0.13	0.40	0.38	0.09	0.34	< 0.02	0.14	< 0.02	< 0.02
MgO	21.8	35.8	23.2	35.9	50.5	51.2	19.0	48.5	20.6	36.0	22.2	22.7
CaO	5.14	0.49	2.41	0.34	0.03	0.02	20.2	0.08	5.55	0.34	2.80	1.57
Na_2O	0.03	0.04	< 0.02	< 0.02	< 0.02	< 0.02	0.80	< 0.02	< 0.02	0.05	< 0.02	< 0.02
K_2O	< 0.01	< 0.01	< 0.01	< 0.01	< 0.01	< 0.01	0.06	< 0.01	< 0.01	< 0.01	< 0.01	< 0.01
Total	100.1	99.6	100.0	100.0	99.4	99.3	99.7	99.2	99.5	99.6	99.2	99.7
Ti	1807.0	8.96	26.8	4.19	0.59	3.22	829.0	54.2	3383.	7.16	56.9	31.2
Rb	0.17	ND	0.09	0.01	0.13	0.14	ND	0.01	0.13	0.15	ND	0.30
Sr	0.77	2.29	1.99	1.67	0.39	0.43	70.7	0.33	0.54	3.11	3.88	28.5
Y	15.9	0.01	0.24	0.00	0.05	0.03	1.36	0.04	18.1	0.01	0.73	0.26
Zr	34.2	0.05	1.52	0.05	0.18	0.14	1.51	0.15	39.4	0.07	2.90	3.96
Nb	1.18	0.01	1.87	0.05	0.02	0.02	0.23	ND	0.49	0.04	0.83	1.35
Ba	0.02	0.03	0.01	0.01	0.11	0.10	1.13	0.04	0.01	0.07	0.06	ND
La	0.11	0.02	0.48	0.01	0.04	0.01	2.18	0.00	0.09	0.03	0.48	2.99
Ce	1.29	0.08	3.55	0.02	0.05	0.03	7.72	0.01	0.81	0.05	3.49	27.9
Pr	0.43	0.01	0.70	0.01	0.03	0.00	1.43	0.00	0.27	0.00	0.67	7.55
Nd	3.28	0.16	3.20	0.04	0.34	0.06	7.25	0.02	2.42	0.00	3.47	45.1
Sm	1.45	0.04	0.24	0.00	0.27	0.07	2.05	0.01	1.66	0.00	0.74	4.04
Eu	0.58	0.00	0.03	ND	0.10	0.02	0.52	0.01	0.69	ND	0.18	0.57
Gd	2.31	0.06	0.20	ND	0.28	0.05	1.24	ND	3.10	0.01	0.61	0.70
Tb	0.48	ND	0.02	0.00	0.04	0.02	0.16	0.00	0.56	ND	0.06	0.15
Dy	3.28	ND	0.10	ND	0.21	0.11	0.67	0.01	3.92	ND	0.24	0.32
Ho	0.72	ND	0.01	0.00	0.03	0.01	0.08	ND	0.76	0.00	0.04	0.06
Er	2.17	ND	0.03	0.03	0.18	0.07	0.19	ND	2.38	ND	0.14	0.15
Yb	2.24	0.00	0.11	ND	0.14	0.05		0.03	2.51	ND	0.25	0.10
Lu	0.36	0.00	0.05	ND	0.05	0.01	0.03	0.00	0.44	ND	0.08	0.05
Hf	1.25	0.00	0.06	0.01	0.22	0.10	0.18	0.01	1.77	0.00	0.06	0.01

control system at Edinburgh University. Positive secondary ions were sputtered by bombardment of the sample with an 8 nA primary beam (beam size about 20–25 μm) of negatively charged oxygen ions. The nominal impact energy of the primary beam on the sample surface was 14.5 keV. An energy offset of 75 ± 20 eV was applied to suppress molecular interferences. Count rates for each element and the background were collected for 50 s. Normally three spots were analysed per sample and then averaged. For smaller samples, however, count rates for 75 s were collected. Corrections were made for the molecular interference of ZrH on Nb, Si + Fe on Rb, BaO on Eu and the LREE oxides on the HREE. Element abundances were normalised to the SRM610 glass standard and concentrations were calculated from intensity ratios against silica. Analyses were verified by analyses of secondary minerals (Dutsen Dushowa garnet of Irving and Frey 1978 and Kilbourne Hole clinopyroxene of Irving and Frey 1984) and glass standards.

Analytical uncertainties are determined by the elemental abundances but also by the ion yields which are different for each element. In general analytical errors for concentrations in the ppm level are small (<1% for concentrations >100 ppm, <10% between 1–10 ppm) but become increasingly large at sub-ppm levels. Concentrations between 1–10 ppb are not reported since errors exceed 50%.

Mineral inclusion chemistry

Garnet

All ten garnets examined are chromian pyropes and belong to the peridotitic diamond inclusion suite. Conventionally, Ca-saturated peridotitic garnets are assigned to the lherzolitic paragenesis (4 garnets) and subcalcic pyropes to the harzburgitic paragenesis (6 garnets). Akwatian garnets may be unusually rich in the knorringite component ($Mg_3Cr_2[SiO_4]_3$) and thus for each paragenesis the pyrope with the highest Cr content (Stachel and Harris, 1997) was included (see Table 1).

The chondrite normalised REE (i.e. REE_N) patterns for these ten garnets compared in Figs. 1 and 2 are clearly distinctive, excluding the two knorringite-rich specimens. The harzburgitic garnets have sinusoidal patterns, beginning at La_N 0.8–2, peaking at Ce_N (2–6) to Nd_N (2–8), then decreasing towards the HREE with a minimum at Ho_N (0.2–0.7), with Lu_N being generally enriched (1.1–6). In one sample (G104-107) the trough at the MREE-HREE transition is pronounced because Gd to Ho were not detected (Fig. 1). Generally the REE_N patterns for harzburgitic garnet inclusions in diamond are very similar to subcalcic garnets in heavy mineral concentrates from the Finsch and Bultfontein kimberlites (Shimizu and Richardson 1987) and to garnets in diamond facies harzburgites (Nixon et al. 1987). Conversely, the chondrite normalised patterns of the lherzolitic garnets show simple HREE enrichment (La_N/Yb_N = 0.02–0.06). The patterns become flat at about 10 times chondrite MREE and HREE (Fig. 2) having risen steeply from La_N (0.4–0.6) and Ce_N concentrations (0.9–2) that are lower than the harzburgitic garnets.

The clear distinction between harzburgitic and lherzolitic garnets is further emphasised for the HFSE, where Ti, Y, Zr, Hf are very low in the harzburgitic garnets and high in the lherzolitic garnets (Fig. 3).

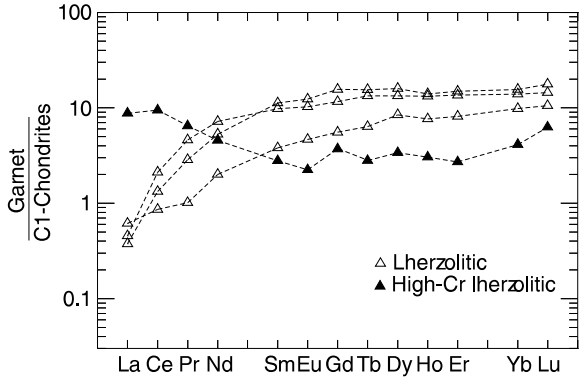

Fig. 2 REE concentrations in lherzolitic garnet inclusions in diamond, normalised to the C1-chondrite composition of McDonough and Sun (1995)

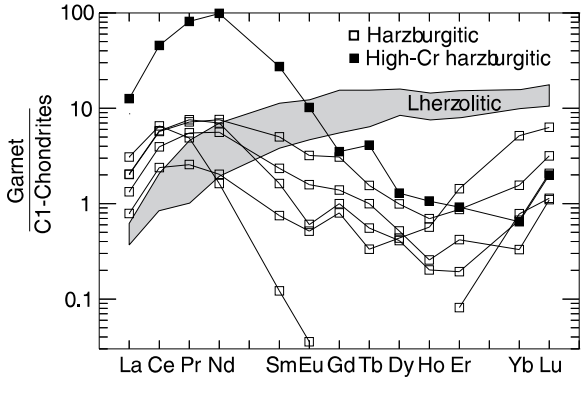

Fig. 1 REE concentrations in harzburgitic garnet inclusions in diamond, normalised to the C1-chondrite composition of McDonough and Sun (1995). Lherzolitic garnet compositions are shown for reference

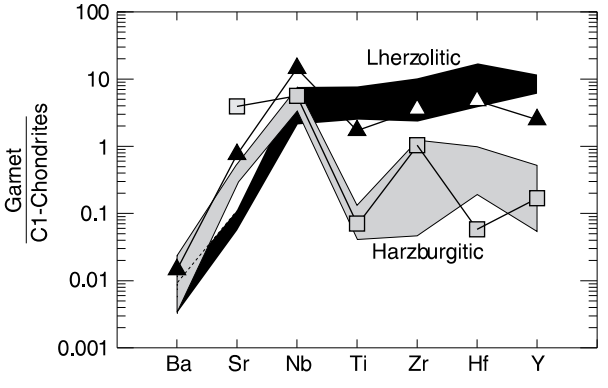

Fig. 3 Compositional fields for trace elements in harzburgitic (*shaded*) and lherzolitic (*black*) garnet inclusions, normalised to the C1-chondrite composition of McDonough and Sun (1995). The high-Cr garnets for each paragenesis (*shaded squares* harzburgitic, *triangles* lherzolitic) are shown separately. Element order corresponds to increasing distribution coefficient between garnet-melt (Green 1994)

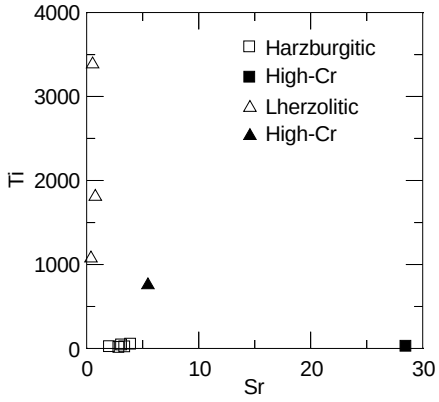

Fig. 4 Sr and Ti concentrations (wt ppm) in garnet inclusions of harzburgitic and lherzolitic paragenesis. Note the clear separation between the parageneses and the increased Sr concentrations for the high-Cr garnets

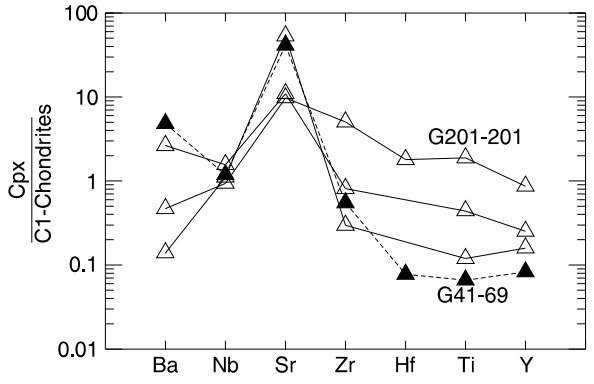

Fig. 5 Trace element concentrations (excluding the REE shown in Fig. 6) in clinopyroxene inclusions, normalised to the C1-chondrite composition of McDonough and Sun (1995). Element order corresponds to increasing distribution coefficient between garnet-melt (Green 1994). Inclusion G41-69 (*black symbols*) is characterised by very high potassium (K_2O 0.72 wt%), which corresponds to the high Ba and Sr concentrations shown here. The HFSE enriched clinopyroxene inclusion G201-201 also shows unusually high concentrations of MREE and HREE in Fig. 6

Strontium concentrations of more than 1 ppm are found only in harzburgitic garnets (Fig. 4, Sr vs. Ti), which is due to preferential partitioning of Sr into clinopyroxene compared to garnet for the lherzolitic paragenesis.

For lherzolitic garnet inclusions the Ti/Zr ratios are very variable (53–120) and one sample (G201-302: Ti/Zr = 86, Ti = 3383 ppm, Zr = 39.4 ppm) actually falls into the fertile garnet lherzolite field as defined by Shimizu and Allègre (1978). According to Shimizu and Richardson (1987) Ti concentrations and Ti/Zr ratios in garnet inclusions from diamonds are low compared to those from garnets in fertile lherzolites, but the values are similar to those in "metasomatized" garnet lherzolite xenoliths, with Ti/Zr of about 1–10 (Shimizu 1975).

Both, the harzburgitic and the lherzolitic high-Cr garnets have distinctively higher LREE contents than the garnets poorer in Cr (Figs. 1 and 2). The lherzolitic garnet (Table 1, G4-3: Cr_2O_3 14.2 wt%) has $LREE_N/HREE_N > 1$ ($La_N/Yb_N = 2.1$) with generally high REE_N enrichment levels compared to the harzburgitic garnets and low MREE and HREE contents for the lherzolitic paragenesis. It has the characteristically high Ti, Y, Zr, and Hf contents of the lherzolitic paragenesis, but atypically high Sr (5.5 ppm) and a faint sinusoidal pattern like the harzburgitic garnets. The high-Cr garnet from the harzburgitic paragenesis (G303-305: Cr_2O_3 20.6 wt%) has the highest knorringite component so far observed in an inclusion in diamond and also is slightly hyper-silicic. Both high Cr and excess in Si (i.e. formation of majoritic garnet) are pressure dependent and thus derivation of this garnet from a greater than usual depth is indicated (equivalent to just below 80 kbar; Stachel and Harris, 1997). It has the sinusoidal REE pattern typical for the harzburgitic paragenesis, but the LREE enrichment reaches far beyond normal levels ($La_N/Yb_N = 20$), peaking at Pr_N (81) and Nd_N (99). The $HREE_N$ (0.6–2) basically represent normal harzburgitic values. Strontium is extremely high (28.5 ppm).

Clinopyroxene

The four clinopyroxenes are lherzolitic chromian augites ("chrome diopsides"). Three have very similar major and minor element compositions (Table 1) with similar La_N/Lu_N ratios (9–170) and La_N (9–15) values. Sample (G41-69) has an unusually high potassium content (K_2O 0.72 wt%), the highest Ba content (Fig. 5) and a significantly different REE pattern, with a La_N/Lu_N ratio of 519 and La_N of 111, representing prominent LREE enrichment (Fig. 6). For all clinopyroxenes the La_N/Lu_N increases with decreasing sodium content. Sample G201-201 has a very smooth REE pattern with a bulge around Nd and sample G50-83 has a steadily decreasing REE pattern while samples G41-69 (K-rich) and G23-29 have spiky HREE (Fig. 6), which are probably due to increasing analytical errors for concentrations close to the detection limits. Sample G201-201 is also different in having generally several times higher concentrations of Zr, Hf, Ti, and Y (Fig. 5). Inter-element correlations

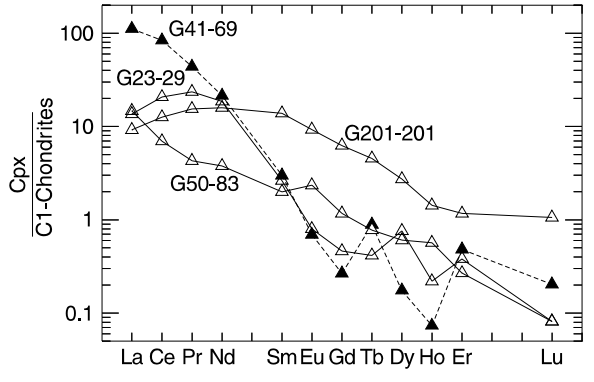

Fig. 6 REE concentrations in clinopyroxene inclusions, normalised to the C1-chondrite composition of McDonough and Sun (1995)

between minor and trace elements seem to exist between Mn and Sr (positive, $r^2 = 0.90$) and between Ni and Ba (negative, $r^2 = 0.89$). The slope from LREE to MREE (La_N/Sm_N) generally decreases with increasing Ni.

Orthopyroxene

Enstatite inclusions (five samples analysed) in the Akwatian diamonds seem to belong entirely to the harzburgitic paragenesis, since they never occur together with clinopyroxene or lherzolitic garnet and have rather low Ca contents (Stachel and Harris, in press). They are not a significant repository for the incompatible trace elements. Concentrations of Ba, Rb, Zr, Y, Hf, Nb and the REE generally were very low (<0.2 ppm) and only Ti (4–9 ppm) and Sr (1.7–4 ppm) detectable at ppm levels.

Olivine

Three olivines of the harzburgitic paragenesis and two of the lherzolitic paragenesis were analysed for trace elements. As with the orthopyroxenes, concentrations for the analysed LILE, HFSE and REE are low (<0.4 ppm), with slightly higher values for Sr (0.3–0.6 ppm) and variable Ti (0.6–54 ppm). As with garnet, the lherzolitic and harzburgitic parageneses can be distinguished in a plot of Sr versus Ti (Fig. 7), with Sr being higher in the harzburgitic and Ti being higher in the lherzolitic paragenesis. For the harzburgitic samples G125-158 and G127-160 REE patterns show strong relative $HREE_N$ enrichment with La_N/Yb_N of 0.18 (G126-158) and 0.10 (G127-160) and $HREE_N$ abundances at about 1.1 and 0.4 respectively. For the third harzburgitic and the two lherzolitic olivines LREE and HREE abundances are extremely low.

Discussion

Calculation of hypothetical melt compositions from mineral data by using K_Ds

To investigate the relative volume and the character of the metasomatic agent it is useful to convert the trace element concentrations of minerals into melt compositions. Ignoring modal relationships, melt compositions can be calculated from mineral analyses for every element just by applying distribution coefficients ($C_{Liquid} = C_{Solid}/K_D$). The internal consistency of the distribution coefficients used and the presence of equilibrium between minerals can be tested by comparing the melt compositions calculated from paired mineral inclusions, e.g. the two pairs of garnet and clinopyroxene which were included in the same diamond (Table 1). In Fig. 8 the chondrite normalised REE patterns for hypothetical melts in equilibrium with these inclusions are shown which were calculated using the distribution coefficients of Fujimaki et al. (1984) derived from kimberlite megacrysts. The same authors also give slightly higher distribution coefficients for garnet and clinopyroxene synthesised at 20.5 kbar, 1150 °C from olivine tholeiite, which yield almost identical patterns. For diamond G50 the melt in equilibrium with clinopyroxene shows a higher degree of REE fractionation than the melt composition calculated from garnet. The different LREE/HREE ratio may be interpreted either as a result of disequilibrium between clinopyroxene and garnet or in terms of distribution coefficients which are not appropriate for the physical conditions of crystallisation of the phases. For diamond G201 (Fig. 8) garnet and clinopyroxene yield identical hypothetical melt compositions. This suggests not only equilibrium between garnet and clinopyroxene in this sample but also indicates the internal consistency of the distribution

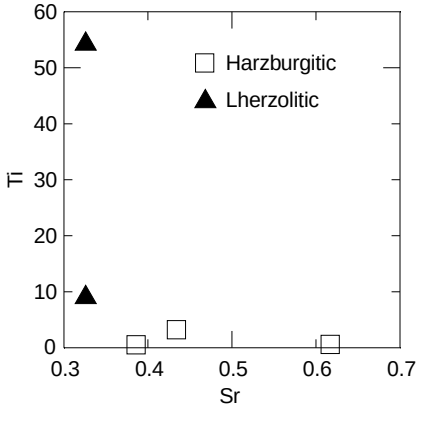

Fig. 7 Sr versus Ti (wt ppm) for olivine inclusions in diamond. As is the case of garnet inclusions the harzburgitic paragenesis is very poor in Ti and the lherzolitic paragenesis is very poor in Sr

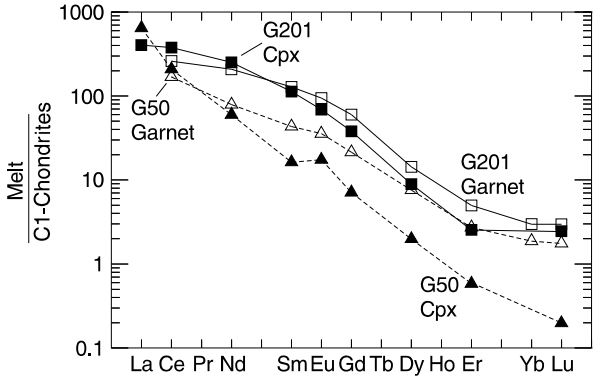

Fig. 8 Melt compositions (chondrite normalised) calculated from the REE concentrations of paired (non-touching) garnet-clinopyroxene inclusions. Whereas in the case of diamond G50 garnet and clinopyroxene indicate different enrichment levels for HREE, the melts calculated from garnet and cpx inclusions in diamond G201 show perfect agreement

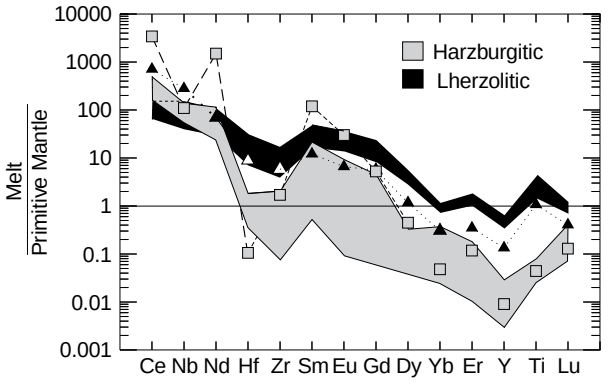

Fig. 9 Compositional fields for melt compositions in equilibrium with garnet inclusions of the harzburgitic and lherzolitic paragenesis. Melt compositions calculated for the high-Cr harzburgitic (*triangles*) and lherzolitic (*squares*) inclusions are shown separately. All compositions are normalised to primitive mantle (Hofmann 1988)

coefficients of Fujimaki et al. (1984) which were used for the calculations.

Figure 9 shows hypothetical melt compositions for all the garnets analysed using the distribution coefficients for REE, Hf and Zr of Fujimaki et al. (1984, megacrysts) together with the values of Green et al. (1989, tholeiitic basalt, run 1132, 25 kbar, 1100 °C) for Ti, Y and Nb. The order of the elements and normalisation coefficients for primitive mantle are taken from Hofmann (1988). Cerium abundance data indicate that the LREE are about 70–400 times enriched in the hypothetical melt compositions in equilibrium with lherzolitic and harzburgitic Akwatian garnets. Note that the bulge within the LREE observed in the harzburgitic garnets (Fig. 1), disappears in the calculated melt compositions (Fig. 9), and thus is only a function of increasing incompatibility towards La. Calculated melts (Fig. 9) show an increase in LREE from lherzolitic to harzburgitic to high-Cr garnets. Harzburgitic melts are characterised by a trough at Hf and Zr, compositions ranging from 2 times primitive mantle to about 0.08 (Zr), with a second trough at Y (down to 0.002 times primitive mantle). The same troughs are also characteristic for the melt composition calculated for the high-Cr harzburgitic garnet, where the depletion in Hf is even more prominent. However, the second trough at Y derived for both types of harzburgitic garnets might be spurious since it is based on an element for which the distribution coefficient was derived using experimental conditions different to those for the REE. Due to the scale used for Fig. 9 the increase in normalised HREE contents from Er towards Lu is not well displayed, whereas reference to Fig. 1 shows a strong slope from Ho or Er to Lu. Very similar REE_N patterns with an upward kink within the $HREE_N$ at Er were found by Nixon et al. (1987) for garnets in diamond facies harzburgite xenoliths from Liqhobong (Lesotho). This positive slope in the HREE might actually represent the original depleted pattern of the harzburgites (with $La_N/Yb_N \ll 1$), before enrichment processes re-introduce LREE and MREE (cf. Bulatov et al. 1991; Shimizu et al. 1996).

The melt compositions for the lherzolitic garnets (Fig. 9) show only a minor trough between Hf and Zr, with Zr being about 10 times that of the primitive mantle. A small trough at Y is also present, but this is mainly due to a positive peak at Ti. The HREE concentrations for the lherzolitic melts are similar to the concentrations in the primitive mantle, i.e. HREE have not been significantly enriched. Assuming that the diamond inclusions actually crystallised from melts similar to those calculated, it implies that either the HREE were retained in the source region of this melt or, if the melt was generated in situ during the introduction of an enriching fluid, that no HREE were contained in that fluid. The high-Cr lherzolitic garnet (Fig. 9) yields a similar picture, although with a steeper LREE/HREE slope. Thus the melt composition calculated for the high-Cr garnet is transitional between the melts in equilibrium with lherzolitic and with harzburgitic garnets. This result indicates that Akwatia Cr-rich lherzolitic garnets crystallised in a chemical environment which is more similar to that of harzburgitic diamonds than to that of "normal" low-Cr lherzolitic garnets.

The high-Cr harzburgitic garnet (Figs. 9 and 10) appears to be in equilibrium with a melt composition with an extreme REE fractionation. Since this garnet is derived from an unusually great depth (just below 80 kbar, Stachel and Harris, 1997), its extreme LREE concentrations may be interpreted as due to an increase in LREE enrichment with increasing depth (i.e. closer to the base of the lithosphere). Alternatively, a decreasing incompatibility of LREE with increasing depth (i.e. increasing P and T) would give the same result. Figure 10 illustrates how the hypothetical melt compositions from these two Cr-rich garnets change, if the distribution coefficients between majoritic garnets and an ultramafic

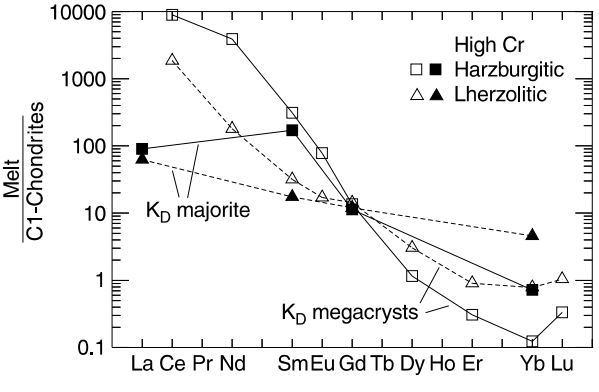

Fig. 10 Melt compositions calculated from REE concentrations in high-Cr garnets using distribution coefficients for kimberlitic megacrysts (*open symbols*) and majoritic garnets (*filled symbols*). The high pressure and temperature distribution coefficients for majoritic garnets result in less fractionated REE patterns for calculated melts, thus possibly relating the extreme REE fractionation in the high-Cr garnets to an unusually deep origin

melt (Yurimoto and Ohtani 1992, run 59, 160 kbar, 1900 °C) are used for the calculation. Application of the majoritic D-values results in a much flatter pattern, with LREE enrichment decreasing from 10 000 times to 100 times chondrite. Compatibility of HREE in contrast, decreases slightly, leading to further flattening of the REE_N pattern. Although the majoritic distribution coefficients derived at 160 kbar, 1900 °C are not appropriate for an inclusion trapped at about 70–80 kbar and 1350–1450 °C, the general conclusion might still be correct, in that changes in garnet composition with increasing depth are a result of changing distribution coefficients.

Comparison with mantle-derived alkaline melts

In the following section the hypothetical melts for lherzolitic and harzburgitic garnets are compared with kimberlites (Dawson 1980) and lamproites (ranges for West Kimberley Province and Argyle, Mitchell and Bergman 1991) as these two rock types represent the most likely candidates capable of producing the observed enrichment. In addition, the kimberlite and lamproite fields generally are similar to the compositions of primitive OIB-like asthenospheric melts assumed to be the agent of mantle metasomatism by Harte et al. (1993), as well as of carbonatitic melts.

The melt compositions calculated from the lherzolitic garnets coincide with the compositional range observed for kimberlites and lamproites (Fig. 11) with slightly lower HREE concentrations for the hypothetical melts. Compatible trace elements (Ni and Cr) also fall within the compositional ranges of kimberlite-lamproite magmas both for lherzolitic and harzburgitic parageneses. The Ni contents of about 3000 ppm in olivines and about 1000 ppm in orthopyroxenes (Stachel and Harris, in press) yield a Ni content of 300–600 ppm for a melt in equilibrium with these inclusions (K_D from Beattie et al. 1991) and from the average Cr contents of clinopyroxenes (about 5500 ppm) a lherzolitic melt has about 1500 ppm (K_D from Hart and Dunn 1993). The resulting Ni/Cr ratio of about 0.1 seems, however, rather low.

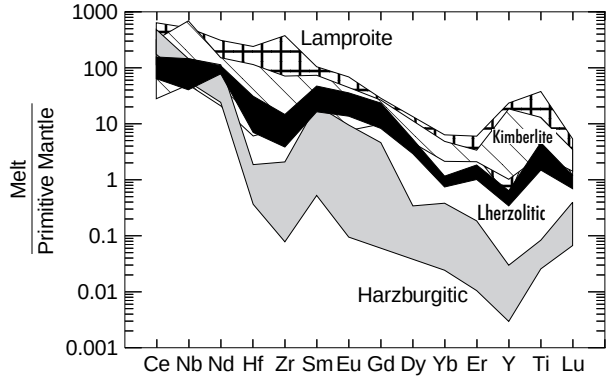

Fig. 11 Compositional fields of melts in equilibrium with harzburgitic and lherzolitic inclusions in diamond compared with the compositional ranges of kimberlites (Dawson 1980) and lamproites (Mitchell and Bergman 1991). Note the similarity of the "lherzolitic melts" with the kimberlite and lamproite fields

Thus crystallisation of the lherzolitic garnet inclusions from a silicate or carbonate melt with trace element compositions similar to lamproites or kimberlites is a distinct possibility. However, possible melt compositions in equilibrium with harzburgitic garnets have REE patterns with slopes too steep to be consistent with crystallisation from a kimberlitic, lamproitic or carbonatitic melt (see also Shimizu and Richardson 1987).

Origin of diamonds and mantle enrichment

The formation of subcalcic, Cr-rich garnets typical for inclusions in diamonds was addressed in experimental work of Bulatov et al. (1991) and Canil and Wei (1992). Bulatov et al. (1991) concluded from experiments in the garnet stability field (50–60 kbar, Green et al. 1986; Brey et al. 1990) that the formation of chromium-rich garnets as result of Cr enrichment during melt extraction was not possible. Melting in the spinel peridotite stability field (5–20 kbar, Bulatov et al. 1991), however, results in residua with high-Cr contents and high Cr/Al ratios. It was suggested, therefore, that Cr-rich, subcalcic garnets are the product of high pressure metamorphism of spinel harzburgites which originated at shallow depth and were then subducted. A similar mechanism has to be evoked for the high-Cr lherzolitic garnets.

This is consistent with the very high Ni contents in olivines of both, the harzburgitic and lherzolitic paragenesis (Stachel and Harris, 1997) which implies that the source for both parageneses must have experienced depletion events of a similar extent, followed by differing degrees of re-enrichment. The present study indicates not only different degrees of re-enrichment for lherzolitic and harzburgitic paragenesis inclusions but also different modes of enrichment. For the lherzolitic paragenesis, diamond formation from low volume melts derived from a previously depleted and re-enriched peridotitic source seems possible. Alternatively, they may have grown in a peridotitic source that experienced strong enrichment from infiltrating melts or fluids. Growth of diamond may be in the solid state or from the low volume melts that formed only during the enrichment event (e.g. by lowering of the peridotite solidus due to the introduction of H_2O or CH_4 rich fluids).

On the basis of the very high $LREE_N$ together with depleted $HREE_N$ required for possible melts in equilibrium with harzburgitic garnets (Fig. 11), Shimizu and Richardson (1987) proposed solid state growth of peridotitic (only subcalcic garnets analysed) diamonds. Shimizu and Richardson (1987) attributed the isotopic and trace element characteristics of peridotitic garnets to "ancient mantle metasomatism". A priori, there are no obvious reasons why incorporation of REE into garnet (in the presence of olivine and orthopyroxene) must

occur at subsolidus conditions and cannot occur when garnet crystallises from a melt. Lack of evidence on the Earth's surface for melts as highly fractionated as those required for harzburgitic diamond inclusions is not a sufficient argument to reject the existence of such melts within the lithospheric mantle. By strictly separating the enrichment and the diamond formation event, Shimizu and Richardson (1987) also provide no explanation as to why diamond should suddenly be formed in an apparently closed system. Decarbonation reactions, as invoked by Shimizu et al. (1989), seem inconceivable to us, since the buffering capacity of peridotite at the pressures in the diamond stability field is far too high (see Eggler 1987 and references therein) and major changes in oxygen fugacity without introduction of a melt or fluid are not to be expected.

If involvement of melts is assumed, the harzburgitic garnet inclusions may have crystallised from low volume partial melts which were formed during an enrichment event related to infiltration of highly fractionated melts or fluids. Whereas the major element characteristics of the inclusions in such a scenario are provided by the melting of the depleted harzburgitic host rocks, the trace element distribution largely reflects the composition of the enriching agent. During crystallisation, in the absence of clinopyroxene, the LREE would be concentrated completely in the harzburgitic garnets. Thus, if re-enrichment of the source and diamond formation are coupled processes, then diamonds and their silicate inclusions could well crystallise from low volume partial melts, if the peridotite solidus is sufficiently lowered during this enrichment event.

Agents for metasomatism

Silicate and carbonate melts and C-H-O rich fluids may be considered as metasomatising agents to account for the enrichment patterns observed in harzburgitic and lherzolitic inclusions in diamond. For the harzburgitic paragenesis the melt or fluid responsible for the re-enrichment has to be very rich in LREE, rich in Rb and Sr (ca. 10–50 times primitive mantle), low in Hf and Zr, and void of HREE, Y and Ti. In addition, the major element characteristics of the Akwatian inclusion suite (Stachel and Harris, 1997) require the introduction of Fe. Chromatographic processes analogous to laboratory methods (Hofmann 1972; Navon and Stolper 1987; Bodinier et al. 1990) which modify an already highly fractionated fluid or melt are capable of producing the required selective LREE enrichment. Stosch and Lugmair (1986) interpret depletions in Hf (and by analogy Zr and Ti) in terms of fluid phase metasomatism rather than silicate melt metasomatism. Menzies et al. (1987) also use low-Ti characteristics as an argument against melt enrichment. Their interpretations thus do not support enrichment by a silicate melt for the source of the harzburgitic diamonds. Harte et al. (1993), however, suggest that infiltrating silicate melts may be Ti depleted due to early stages of ilmenite fractionation. Infiltration of silicate melts into subsolidus peridotite requires H_2O-rich compositions since all other melts would solidify rapidly. According to Harte et al. (1993) mantle metasomatism by such silicate melts is characterised by high Ba, Sr, and Zr concentrations. These enrichment processes would cause growth of minerals such as ilmenite, biotite or K-richterite which are not common as inclusions in diamond.

The capability of C-H-O-rich fluids to cause the observed enrichment is difficult to assess, since only limited data are available on the solubility of major and trace elements. Meen et al. (1989) demonstrated that CO_2-rich fluids have very low solubilities for REE at mantle conditions and thus are inapt as agents for LREE enrichment. Eggler's review (1987) indicates that H_2O fluids at high pressures are well capable of causing REE enrichment, but have low solubilities for Sr, Ba and major elements. This seems to be inconsistent with the Sr and Fe enrichment observed for the harzburgitic inclusions. High pressure experiments (Stalder et al. 1997) on the partitioning of trace elements between garnet or cpx and a hydrous fluid showed that the solubility in the fluid decreases from LFSE to HFSE and accordingly from LREE to HREE. Solubility data for CH_4-rich fluids are not available.

Infiltration of peridotite by CO_2-rich fluids is also inconsistent with dihedral angle data (Watson et al. 1990) since the observed high values prevent the interconnectivity of the fluid necessary for penetration along grain edges. More importantly, CO_2-rich fluids are unstable under the pressures in the diamond stability field, since CO_2 reacts with peridotite at subsolidus conditions to form carbonate phases (Brey et al. 1983). The same would apply for a CO_2-rich melt percolating through mantle peridotite at subsolidus conditions. Thus, a percolative process involving a CO_2-rich fluid or melt is not a feasible explanation for the observed REE fractionation in the harzburgitic inclusions.

Neither silicate melts nor CO_2-rich fluids seem to be likely agents for the observed metasomatism which leaves only Ti-poor carbonatitic melts or, depending on the oxygen fugacity, H_2O- or CH_4-H_2-rich fluid phases, as probable candidates to explain the observed LREE enrichment in harzburgitic inclusions. Fluids rising from the deep mantle may indeed be reduced (Wyllie 1980; Foley 1988; Ballhaus 1995), so that a situation may be envisaged where the infiltration of CH_4-H_2-rich fluids into more oxidised lithospheric peridotite initiates a redox melting process and as a consequence the precipitation of carbon as diamond (Taylor and Green 1989).

In contrast to such reduced fluids rising from the deep mantle, fluids emanating from intrusions into subsolidus peridotite would be water rich after losing their possible CO_2 content by carbonation reactions. However, metasomatism by infiltrating C-H-O-rich fluids (because of high dihedral angles in subsolidus dunites) seems only to operate near the peridotite solidus (Watson et al. 1990; Nielson and Wilshire 1993). Yet, Watson et al. (1990)

showed that dihedral angles for H_2O-rich fluids are reduced considerably with increasing pressure and temperature. Thus, at the *P-T* conditions within the diamond stability field permeability of peridotite for H_2O-rich fluids seems conceivable at subsolidus conditions. In peridotite with a strongly sheared texture, subsolidus migration of H_2O-rich fluids along grain boundaries would be considerably facilitated.

Equilibration temperatures and peridotite solidus

If crystallisation of diamond in the presence of a melt is a viable possibility temperatures of formation of diamond should be compared with the position of the peridotite solidus. Garnet-opx equilibria for Akwatian inclusions yield *P-T* conditions of crystallisation of diamond along a conductive geotherm corresponding to 40–42 mW/m^2 surface heat flow. This geothermal gradient is similar to that determined from garnet-opx pairs (Fig. 12) in diamonds from southern African localities (Stachel and Harris, 1997, and references therein). Olivine-garnet pairs were used to calculate temperatures (O'Neill and Wood 1979) as a function of pressure for 25 Akwatian diamonds. The shaded region in Fig. 12 marks the intersection of the 1σ range of the calculated temperatures with the 40 to 42 mW/m^2 heatflow gradients. The upper pressure limit of 80 kbar in Fig. 12 is the highest possible pressure estimated from the slightly hyper-silicic chromium-rich garnet (see above). Also shown are the solidi of lherzolite-H_2O/CO_2-H_2O (from Wyllie 1989, Fig. 10.6) and for harzburgite-H_2O (from Wyllie 1987, Fig. 318, extrapolated to pressures >70 kbar).

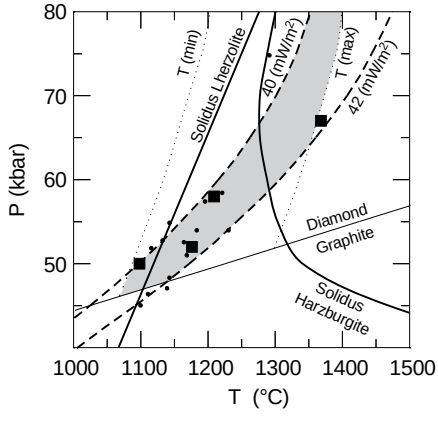

Fig. 12 *P-T* conditions calculated from garnet-opx equilibria (Brey and Köhler 1990; Harley 1984) for diamonds from Akwatia (*filled squares*) and other locations world-wide (*small circles*). The *dashed lines* give the conductive shield geotherms for 40 and 42 mW/m^2 surface heat flow (calculated after Pollack and Chapman 1977). The *dotted lines* indicate the 1σ-range [*T*(min), *T*(max)] of temperatures (O'Neill and Wood 1979; O'Neill 1980) calculated for various pressures for 25 Akwatian diamonds containing olivine-garnet pairs (Stachel and Harris, 1997). The *shaded area* represents the field where the garnet-olivine temperatures coincide with the geothermal gradients indicated by the garnet-opx geothermobarometry. In addition, the solidi in the presence of C-H-O (Wyllie 1987, 1989) for harzburgite and lherzolite and the graphite diamond phase boundary (Kennedy and Kennedy 1976) are shown

Most estimated *P-T* conditions for diamond formation plot at or above the lherzolite-H_2O/CO_2-H_2O solidus. Formation of low volume partial melts during metasomatism of a lherzolitic lithospheric upper mantle by H_2O-rich fluids or through redox reactions with CH_4-H_2-rich fluids seems inevitable. Conditions at or above the lherzolite solidus would also allow infiltration of and equilibration with kimberlitic, lamproitic or carbonatitic melts.

The harzburgite-H_2O solidus lies at higher temperatures and partial melting would occur only at temperatures above about 1300 °C (for the given geothermal gradient). If crystallisation of diamond is linked to the metasomatic event recorded in its inclusions, it must occur at subsolidus conditions by an agent that is capable not only of causing the extreme LREE enrichment but is also able to precipitate diamond. Carbon dioxide-rich fluids can be excluded, so that carbon precipitation must occur by redox reactions involving methane-rich fluids. These fluids are highly enriched in LREE due to "chromatographic" type interaction with peridotitic wall rocks.

Concluding remarks

From trace element abundances in diamond inclusions and from modelling the hypothetical trace element composition of coexisting melts, differing scenarios for the growth of diamonds with lherzolitic and harzburgitic inclusions have been deduced:

1. Lherzolitic garnets would be consistent with crystallisation from kimberlitic, lamproitic, or carbonatitic melts. The *PT* estimates indicate that the inclusions were trapped at temperatures at around or above the lherzolite-H_2O/CO_2-H_2O solidus and REE enrichment occurred from percolating melts. Alternatively, percolating CH_4- or H_2O-rich fluids would lower the solidus sufficiently to induce partial melting and diamond crystallisation in the presence of melt.

2. Harzburgitic garnets do not seem to be consistent with crystallisation from normal kimberlitic, lamproitic or carbonatitic melts because of their extremely fractionated REE patterns. For diamonds of the harzburgitic paragenesis the solidus temperature (harzburgite-H_2O) of their source is higher than the majority of observed equilibration temperatures. Methane-rich fluids are the most likely metasomatising agents from which diamonds precipitate in a process analogous to the redox melting model of Taylor and Green (1989). A "chromatographic" type fractionation process favoured the selective LREE enrichment (Navon and Stolper 1987; Bodinier et al. 1990) which was transposed onto the diamond inclusions.

Carbon isotopic compositions favour precipitation of diamond from CH_4 (Deines 1980; Kirkley et al. 1991) as

opposed to CO_2, since CH_4 yields the observed mode in $\delta^{13}C$ of about –5‰. Based mainly on the carbon isotopic composition of diamond, the composition and abundance of sulphide inclusions, and the presence of water in the diamond structure, Deines and Harris (1995) suggested crystallisation of diamond from CH_4-rich fluids containing sulphur, other volatiles and little of the components of silicates. The comparatively low concentrations of constituents of silicate phases in such a fluid would account for the fairly large variations in the major element composition of inclusions within a single diamond suite, compared to the very narrow distribution of the carbon isotopic composition, as is the case, for example, for Akwatia (Stachel and Harris, 1997). A C-H-O fluid could also account for the rather large variations in the REE contents and patterns of multiple garnet inclusions in the same diamond (Shimizu and Sobolev 1995). The chemistry of silicate inclusions in diamond would be the result of the composition of the introduced fluid and the chemical interaction with peridotitic wall rock. The differences between lherzolitic and harzburgitic paragenesis inclusions may simply result from the interaction of similar fluids with different peridotitic wall rocks.

Acknowledgements For his help on the ion microprobe and his continuous good humour we are grateful to John Craven. Gerhard Brey, Steve Foley, Ben Harte and Richard Hinton are thanked for helpful discussions and suggestions on the interpretation of our results. T.S. gratefully acknowledges funding by the European Union under the Marie Curie Fellowship scheme. DeBeers Consolidated Diamond Mines Ltd. are also thanked for financial support of the project.

References

Ballhaus C (1995) Is the upper mantle metal-saturated? Earth Planet Sci Lett 132: 75–86

Beattie P, Ford C, Rusell D (1991) Partition coefficients for olivine-melt and orthopyroxene-melt systems. Contrib Mineral Petrol 109: 212–224

Bodinier JL, Vasseur G, Vernières J, Dupuy C, Fabriès J (1990) Mechanisms of mantle metasomatism: geochemical evidence from the Lherz orogenic peridotite. J Petrol 31: 597–628

Brey G, Köhler T (1990) Geothermobarometry in four-phase lherzolites. II. New thermometers and practical assessment of existing thermometers. J Petrol 37: 1353–1378

Brey G, Brice WR, Ellis DJ, Green DH, Harris KL, Ryabchikov ID (1983) Pyroxene-carbonate reactions in the upper mantle. Earth Planet Sci Lett 62: 63–74

Brey G, Köhler T, Nickel KG (1990) Geothermobarometry in four-phase lherzolites. I. Experimental results from 10 to 60 kbar. J Petrol 31: 1313–1352

Bulatov V, Brey GP, Foley SF (1991) Origin of low-Ca, high-Cr garnets by recrystallization of low-pressure harzburgites. Fifth Int Kimberlite Conf, Araxá (Brazil), Extended Abstr, CPRM Spec Publ 2/91: 29–31

Canil D, Wei KJ (1992) Constraints on the origin of mantle-derived low Ca garnets. Contrib Mineral Petrol 109: 421–430

Dawson JB (1980) Kimberlites and their xenoliths. Springer, Berlin Heidelberg New York

Deines P (1980) The carbon isotopic composition of diamonds: relationship to diamond shape, color, occurrence and vapor composition. Geochim Cosmochim Acta 44: 943–961

Deines P, Harris JW (1995) Sulfide inclusion chemistry and carbon isotopes of African diamonds. Geochim Cosmochim Acta 59: 3173–3188

Eggler DH (1987) Solubility of major and trace elements in metasomatic fluids: experimental constraints. In: Menzies MA, Hawkesworth CJ (eds) Mantle metasomatism. Academic Press, London, pp 21–41

Foley SF (1988) The genesis of continental basic alkaline magmas – an interpretation in terms of redox melting. J Petrol Spec Lithosphere Issue: 139–161

Fujimaki H, Tatsumoto M, Aoki K (1984) Partition coefficients of Hf, Zr, and REE between phenocrysts and groundmasses. J Geophys Res 89 Suppl: B662–B672

Green DH, Falloon TJ, Brey GP, Nickel KG (1986) Peridotite melting to 6 Gpa and genesis of primary mantle-derived magmas. Fourth Int Kimberlite Conf, Perth (Australia), Extended Abstr: 181–183

Green TH (1994) Experimental studies of trace-element partitioning applicable to igneous petrogenesis – Sedona 16 years later. Chem Geol 117: 1–36

Green TH, Sie SH, Ryan CG, Cousens DR (1989) Proton microprobe-determined partitioning of Nb, Ta, Zr, Sr and Y between garnet, clinopyroxene and basaltic magma at high pressure and temperature. Chem Geol 74: 201–216

Harley SL (1984) An experimental study of the partitioning of iron and magnesium between garnet and orthopyroxene. Contrib Mineral Petrol 86: 359–373

Harte B, Hunter RH, Kinny PD (1993) Melt geometry, movement and crystallisation, in relation to mantle dykes, veins and metasomatism. Philos. Trans R Soc London A 342: 1–21

Hart SR, Dunn T (1993) Experimental cpx/melt partitioning of 24 trace elements. Contrib Mineral Petrol 113: 1–8

Hofmann AW (1972) Chromatographic theory of infiltration metasomatism and its application to feldspars. Am J Sci 272: 69–90

Hofmann AW (1988) Chemical differentiation of the Earth: the relationship between mantle, continental crust, and oceanic crust. Earth Planet Sci Lett 90: 297–314

Irving AJ, Frey FA (1978) Distribution of trace elements between garnet megacrysts and host volcanic liquids of kimberlitic and rhyolitic composition. Geochim Cosmochim Acta 42: 771–787

Irving AJ, Frey FA (1984) Trace element abundances in megacrysts and their host basalts: constraints on partition coefficients and megacryst genesis. Geochim Cosmochim Acta 48: 1201–1221

Kennedy CS, Kennedy GC (1976) The equilibrium boundary between graphite and diamond. J Geophys Res 81: 2467–2470

Kirkley MB, Gurney JJ, Otter ML, Hill SJ, Daniels LR (1991) The application of C isotope measurements to the identification of the sources of C in diamonds: a review. Appl Geochem 6: 477–494

McDonough WF, Sun S-S (1995) The composition of the Earth. Chem Geol 120: 223–253

Meen JK, Eggler DH, Ayers JC (1989) Experimental evidence for very low solubility of rare-earth elements in CO2-rich fluids at mantle conditions. Nature 340, No 6231: 301–303

Menzies MA, Rogers N, Tindle A, Hawkesworth CJ (1987) Metasomatic and enrichment processes in lithospheric peridotites, an effect of asthenosphere-lithosphere interaction. In: Menzies MA, Hawkesworth CJ (eds) Mantle metasomatism. Academic Press, London, pp 313–364

Mitchell RH, Bergman SC (1991) Petrology of lamproites. Plenum, New York

Navon O, Stolper E (1987) Geochemical consequences of melt percolation: the upper mantle as a chromatographic column. J Geol 95: 285–307

Nielson JE, Wilshire HG (1993) Magma transport and metasomatism in the mantle: a critical review of current models. Am Mineral 78: 1117–1134

Nixon PH, van Calsteren PWC, Boyd FR, Hawkesworth CJ (1987) Harzburgites with garnets of diamond facies from Southern African kimberlites. In: Nixon PH (ed) Mantle xenoliths. J Wiley and Sons, Chichester, pp 523–533

O'Neill HStC (1980) An experimental study of the iron-magnesium partitioning between garnet and olivine and its calibration as a geothermometer: corrections. Contrib Mineral Petrol 72: 337

O'Neill HStC, Wood BJ (1979) An experimental study of the iron-magnesium partitioning between garnet and olivine and its calibration as a geothermometer. Contrib Mineral Petrol 70: 59–70

Pollack HN, Chapman DS (1977) On the regional variation of heat flow, geotherms, and lithospheric thickness. Tectonophysics 38: 279–296

Richardson SH, Gurney JJ, Erlank AJ, Harris JW (1984) Origin of diamonds from old continental mantle. Nature 310: 198–202

Richardson SH, Harris JW, Gurney JJ (1993) Three generations of diamonds from old continental mantle. Nature 366: 256–258

Shimizu N (1975) Rare earth elements in garnets and clinopyroxenes from garnet lherzolite nodules in kimberlites. Earth Planet Sci Lett 25: 26–32

Shimizu N, Allègre CJ (1978) Geochemistry of transition elements in garnet lherzolite nodules in kimberlites. Contrib Mineral Petrol 67: 41–50

Shimizu N, Richardson SH (1987) Trace element abundance patterns of garnet inclusions in peridotite-suite diamonds. Geochim Cosmochim Acta 51: 755–758

Shimizu N, Sobolev NV (1995) Young peridotitic diamonds from the Mir kimberlite pipe. Nature 375: 394–397

Shimizu N, Gurney JJ, Moore R (1989) Trace element geochemistry of garnet inclusions in diamonds from the Finsch and Koffiefontein kimberlite pipes. 28th Int Geol Congr Workshop Diamonds Extended Abstr: 100–101

Shimizu N, Pokhilenko NP, Boyd FR, Pearson DG (1996) Comparative trace element geochemistry of peridotite xenoliths from Siberian and Kaapvaal craton roots. Goldschmidt Conf Heidelberg 1996 J Conf Abstr 1: 565

Stachel T, Harris JW (1997) Syngenetic inclusions in diamond from the Birim field (Ghana) – a deep peridotitic profile with a history of depletion and re-enrichment. Contrib Mineral Petrol 127: 336–352

Stalder R, Jenner GA, Foley SF, Brey GP (1997) The role of aqueous fluids in trace element fractionation in subduction zone processes: evidence from experiments at 3 to 5.5 GPa and 1000 °C. SOTA '97, Island Arc Magma Genesis Workshop Geol Soc Aust Abstr 45: 85–87

Stosch HG, Lugmair GW (1986) Trace element and Sr and Nd isotope geochemistry of peridotite xenoliths from the Eifel (West Germany) and their bearing on the evolution of the subcontinental lithosphere. Earth Planet Sci Lett 80: 281–298

Taylor WR, Green DH (1989) The role of reduced C-O-H fluids in mantle partial melting. In: Ross J (ed) Kimberlites and related rocks: their composition, occurrence, origin and emplacement. GSA Spec Publ No 14, vol 1, Blackwell, Carlton, pp 592–602

Watson EB, Brenan JM, Baker DR (1990) Distribution of fluids in the continental mantle. In: Menzies MA (ed) Continental mantle. Oxford Monogr Geol Geophys 16, pp 111–125

Wyllie PJ (1980) The origin of kimberlites. J Geophys Res 85: 6902–6910

Wyllie PJ (1987) Metasomatism and fluid generation in mantle xenoliths. In: Nixon PH (ed) Mantle xenoliths. J Wiley and Sons, Chichester, pp 609–621

Wyllie PJ (1989) The genesis of kimberlites and some low-SiO_2, high-alkali magmas. In: Ross J (ed) Kimberlites and related rocks: their composition, occurrence, origin and emplacement. GSA Spec Publ No 14, vol 1, Blackwell, Carlton, pp 603–615

Yurimoto H, Ohtani E (1992) Element partitioning between majorite and liquid: a secondary ion mass spectrometer study. Geophys Res Lett 19: 17–20